Available online at www.sciencedirect.com
SCIENCE DIRECT®
Journal of Molecular Catalysis A: Chemical 211 (2004) 179–189
JOURNAL OF MOLECULAR CATALYSIS A: CHEMICAL
www.elsevier.com/locate/molcata

Acid–base properties of NiW/Al_2O_3 sulfided catalysts: relationship with hydrogenation, isomerization and hydrodesulfurization reactions

D. Zuo [a,b], D. Li [a], H. Nie [a], Y. Shi [a], M. Lacroix [b], M. Vrinat [b,*]

[a] *Research Institute of Petroleum Processing — SINOPEC, 18 Xueyuan Road, Beijing 100083, PR China*
[b] *Institut de Recherches sur la Catalyse, 2 Av. Einstein, 69626 Villeurbanne Cedex, France*

Received 4 July 2003; received in revised form 25 August 2003; accepted 7 October 2003

Abstract

NiW/Al_2O_3 catalysts with constant tungsten loading and variable amounts of nickel were tested in the hydrodesulfurization (HDS) of thiophene and 4,6-dimethyldibenzothiophene (4,6-DMDBT), and in the isomerization of *o*-xylene. Introduction of Ni promotes the overall activity for both thiophene HDS and 4,6-DMDBT HDS, but the synergy is more pronounced for the former. Such effect has been analyzed on the basis of the two reaction routes generally involved in the HDS mechanism: direct desulfurization (DDS) and hydrogenation (HYD). Moreover there is a parallelism between the increase of the DDS route and the isomerization of *o*-xylene, proof of a correlation between the promoter content and some acidic properties of the sulfides.

HREM examinations indicated few effect of the promoter over the morphology of the sulfide phase and XPS studies show that Ni is mainly present in the form of "NiWS" phase at the low Ni/[Ni + W] ratio, while separate Ni sulfide is formed at the high one. Such an evolution of Ni species varying with Ni content is responsible to the changes in catalytic activity and selectivity.

Keywords: Thiophene; 4,6-Dimethyldibenzothiophene; Xylenes; NiW/Al_2O_3; Hydrodesulfurization; Hydrogenation; Isomerization

1. Introduction

In order to protect the urban areas, environmental legislation has been adopted to limit the sulfur level in diesel fuel and the need to produce extremely clean fuel is continually increasing. For example, the sulfur content of light oils has been imposed to be 500 ppm in EEC since 2000, and in Japan since 1997. More severe specifications with a sulfur content of 350 ppm is currently practiced, and a sulfur content as low as 10 ppm is being proposed in Europe in the near future. Very deep conversion of sulfur compounds is therefore of prime importance, and such an objective needs the development of more active catalysts, and a better knowledge of the hydrodesulfurisation (HDS) mechanism.

Concerning such ultra deep HDS, it is now well established that among all the sulfur containing compounds present in gas oil, alkyldibenzothiophenes with alkyl groups near the sulfur atom (fourth and sixth positions) are the most refractory [1–4], and numerous studies have been carried out in the last few years over metal complexes and heterogeneous catalysts to better understand why such species are the most difficult to eliminate [5–10]. In a previous work based on a kinetic approach using competitive HDS experiments [8], we assumed that, after adsorption via an aromatic ring, the dibenzothiophene molecule is first hydrogenated to dihydrodibenzothiophene in agreement with the old proposal of Singhal et al. [11]. Then this unstable intermediate is further transformed along two pathways by hydrogenation (HYD) into tetrahydro-, and hexahydro-dibenzothiophene or by desulfurization according to an elimination mechanism leading to biphenyl derivatives. For these two pathways commonly designated respectively as "hydrogenation pathway" and "direct hydrogenolysis" the transformation can be therefore decomposed into H addition steps and C–S bond cleavage by elimination (or E_2) steps. Such a mechanism could well explain the various intermediates observed during the transformation of a non-symmetrical molecule as the 4-methyl-dibenzothiophene [12].

As regard to the formation of these dihydro intermediates in DBT-like molecules, it has been kinetically demonstrated

* Corresponding author. Tel.: +33-4-72-44-5323; fax: +33-4-72-44-5399.
E-mail address: michel.vrinat@catalyse.cnrs.fr (M. Vrinat).

1381-1169/$ – see front matter © 2003 Elsevier B.V. All rights reserved.
doi:10.1016/j.molcata.2003.10.018

[13] to proceed first by addition of an H atom with a hydride character and then by the addition of a proton adsorbed on a sulfur anion of the catalytic surface, in the same sequence that was proposed by Kasztelan and Guillaume for toluene HYD [14]. The elimination reaction could therefore happen if some basic species of the catalytic surface is closed to the dihydro-intermediate. Selectivity toward the direct desulfurization (DDS) or the HYD into tetrahydro-, and hexahydro-dibenzothiophene is therefore controlled by the basicity of the anion, but also by the steric hindrance induced by the alkyl groups as illustrated in the work of Macaud et al. [10] in which numerous alkyldibenzothiophenes with more or less voluminous substituents were compared. Importance of the dihydroderivatives as intermediates in the HDS of dibenzothiophene-type compounds has been reconsidered later [15,16] and has confirmed the previous proposals. However, even if it has been observed for a long time that HYD/hydrogenolysis selectivity was different for promoted and un-promoted molybdenum based catalysts, that point was solely recently addressed by comparison of the catalytic properties of two series of Ni or Co promoted Mo/alumina catalysts having different Ni or Co contents, in dibenzothiophene HDS [17]. The authors concluded that a modification of the basic and nucleophilic properties of the catalysts by promoter addition must be considered to account for the effect of the promoter on the rate of the DDS reaction. Proof of such an effect of the promoter over acid–base properties of the sulfide phase and consequently over the enhancement of the C–S bond cleavage is therefore a key point for the future development of more active catalysts. This could be done by comparison of such a series of catalysts not only in HDS reaction, but also in a reaction such as isomerization which is well recognized to be deeply related to the Bronsted acidity of the catalysts. This was the main objective of this work. Moreover, taking into account the importance of the HYD function of the catalyst in the transformation of the refractory compounds, we chose to study NiW catalysts, which have been far less investigated.

The aim of this paper was therefore to examine HDS and isomerization in a series of NiW catalysts prepared over the same support, with the same tungsten content but increasing Ni/W ratios. Moreover in order to control the increase of activity that could be mainly correlated to promoter content, the catalysts were characterized by XPS and STEM. Attention was not only focused on activity but also on selectivities, and an attempt was made to confirm the HDS mechanism.

2. Experimental

2.1. Catalyst preparation

The NiW catalysts were prepared by co-impregnation of an industrial γ-Al_2O_3 (extrudates, 270 m^2/g) using the incipient wetness method with an aqueous solution of the appropriate amount of ammonium metatungstate hydrate [$(NH_4)_6W_{12}O_{39}$ H_2O] and nickel nitrate hexahydrate [$Ni(NO_3)_2$ $6H_2O$]. After impregnation, the catalyst was oven dried at 393 K for 3 h and then calcined in an air flow at 723 K for 4 h. All the samples were prepared with a constant amount of W (corresponding to 3.2 W atoms per nm^2 of support) and variable concentration of Ni. They were characterized by the Ni/(Ni + W) atomic ratio denoted hereafter by *r* and indicated in the text by NiW(r).

2.2. Chemical analysis

The elemental contents of Ni, W, and Al in oxidic catalysts were determined by plasma atomic emission method (ICP). Some standardized dissolution procedures were necessary to dissolve the sample. The method depends on the nature of the elements to be analyzed. For W analysis, the sample was corroded with a mixture of H_2SO_4 and HNO_3 by heating to 523–573 K.

2.3. BET surface area measurement

Surface area, pore volume and pore size distribution were obtained from N_2 adsorption–desorption isotherms using the conventional BET and BJH methods. The samples were first dried at 393 K for 2 h, and subsequently outgased at 573 K under vacuum before recording the isotherm.

2.4. XPS analysis

The sulfided samples were transferred into a glove box without air exposure. The samples were pressed on an indium foil attached to the sample holder and transported into the preparation chamber of the XPS machine. The XPS spectra were recorded on a VG Instrument type ESCALAB 200R system. The sample excitation was done by Al Kα X-rays (1486.6 eV). Peak shifts due to charging of the samples were corrected by taking the Al 2p line of Al_2O_3 at 74.0 eV as a reference.

2.5. Transmission electron microscopy (TEM)

High resolution electron microscopy (HREM) examinations were performed with a JEOL 2010 (200 kV) instrument equipped with a Link ISIS micro-analysis system. Its resolution is 0.195 nm. Freshly sulfided catalyst sample was ultrasonically dispersed in an ethanol solution at room temperature and the suspensions were collected on a carbon-coated copper grid.

In the sulfided state, alumina-supported W catalysts exhibit WS_2 slabs building a layered structure. The average number of layers per stack and the average stack length were calculated from examination of more than 500 particles, according to the first moment of the distribution:

$$\bar{L} = \frac{\sum_{i=1}^{n} n_i l_i}{\sum_{i=1}^{n} n_i}$$

and

$$\bar{N} = \frac{\sum_{i=1}^{n} n_i N_i}{\sum_{i=1}^{n} n_i}$$

Where l_i is the length of slab-particle i, n_i the number of particles with a l_i length or N_i layers, and N_i the number of layers in the particle i.

2.6. Thiophene hydrodesulfurization

The oxidic catalysts were crushed and sieved to 80–125 μm. Sulfidation was performed ex-situ in a flowing gas mixture containing 10 vol.% H_2S in H_2 at 673 K for 4 h. The heating rate was 10 K/min and the H_2S/H_2 flow rate mixture was 66.7 ml/min. The sulfided catalysts were cooled down to room temperature, flushed with N_2 for half an hour and kept under argon for use.

The catalytic activity tests for thiophene HDS were carried out in a typical micro-reactor apparatus in a continuous operating mode and at atmospheric pressure. Appropriate amount of catalyst was used in order to limit the conversion lower than 20%. The thiophene was introduced into the reactor by flowing H_2 (50 ml/min) through a thiophene saturator maintained at 273 K. The reaction was running at 573 K overnight until the conversion became stable, and after being evaluated in the range from 553 to 593 K. Products were analyzed using on-line gas chromatography equipped with a FID detector and a 30 m × 0.53 mm capillary column coated with a homogeneous layer of Al_2O_3 deactivated by Na_2SO_4.

The rate of thiophene transformation was calculated as $Rs = (F/m)\,X$, where Rs is the specific rate expressed as moles of thiophene transformed per second and per gram of catalyst, F is the molar flow rate of reactant, m represents the mass of catalyst and X is the fractional thiophene conversion.

2.7. 4,6-DMDBT hydrodesulfurization

4,6-DMDBT HDS was carried out in a stirred slurry tank reactor (300 ml) operating in batch mode. In each run, the autoclave was charged with 80 ml of dodecane containing 250 mg reactant and 250 mg *n*-hexadecane (Aldrich, 99%) used as an inner standard. Appropriate amount of freshly sulfided catalyst was added rapidly to the reaction mixture in order to avoid exposure to air. The reactor was first flushed with nitrogen and heated under stirring to reach the reaction temperature (573 K), and then hydrogen was introduced to the pressure of 5 MPa. This moment was considered as the starting point.

Samples of the reaction mixture were taken periodically in the course of the reaction and analyzed by a gas chromatograph (HP 4890A) equipped with a HP-5 column (5% phenylmethylsilicone, 30 m × 0.32 mm) and a FID detector.

The catalytic activity was expressed by the initial specific rate (moles of 4,6-DMDBT transformed per second and per gram of catalyst).

2.8. o-Xylene isomerization reaction

o-Xylene isomerization reaction was performed on a high pressure stainless steel fixed bed micro-flow reactor. For the activity test, 0.15–0.2 g of catalyst was in-situ sulfided with a solution of 10 wt.% CS_2 in cyclohexane at a flow rate of 0.2 ml/min, under 573 K, 4.14 MPa H_2 pressure and a H_2 flow rate of 400 ml/min for 2.5 h. Then the reactor was switched to the reactant feed (40 wt.% *o*-xylene, and 60 wt.% cyclohexane) with a flow rate of 0.1 ml/min under the same hydrogen atmosphere. The reaction was performed at 573 K. The liquid samples were periodically collected and analyzed by GC–FID (Perkin-Elmer 8000) on a 30 m × 0.25 mm SE54 capillary column with a temperature program: 363 K for 2 min, 6 K/min to 443 K and then 10 K/min to 513 K holding for 6 min. The products were qualitatively identified by GC–MS.

3. Results

3.1. Catalysts composition

The contents of Ni and W in the catalysts and some textural properties are listed in Table 1. The BET surface area of pure alumina is 270 m^2/g whereas a diminution of textural properties is already observed as far as W is introduced (see Table 1). However a further introduction of Ni does not provokes any more significant diminution of surface area. Therefore we can consider the BET area as a constant for our purpose of studying the effect of the Ni concentration on the catalytic properties of the NiW system.

3.2. XPS analysis

3.2.1. Surface species of sulfided NiW/Al_2O_3 catalysts

The XPS spectra showing W_{4f} levels for NiW/Al_2O_3 catalysts sulfided at 673 K are presented in Fig. 1a for the various samples, and example of the decomposition is given in Fig. 1b for the catalyst NiW (0.60). Binding energies of W, Ni and S are summarized in Table 2. The observed binding energies are in agreement with those previously published on similar W and NiW catalysts ([18] and references therein). Indeed, XPS of S_{2p} on the sulfided NiW/γ-Al_2O_3 catalysts exhibits only one peak at about 161.6 eV, which corresponds to S^{2-}. The absence of any signal at 169 eV indicates that no oxidation of the catalysts occurred during the transfer of the solid from the sulfiding reactor to the XPS machine. The W_{4f} doublet lines at 32 and 34.1 eV correspond to W^{4+} species in a WS_2-like structure while bands at 35.5, and 37.5 eV are the fingerprints of W^{6+} in an oxygen environment (WO_3).

In order to estimate the fraction of sulfided W^{4+} species present on the various catalysts, the W_{4f} XPS signals were fitted assuming the coexistence of both W^{6+} and W^{4+} species (see Fig. 1b). Data are reported in Table 3.

Table 1
Composition and physical properties of the oxidic Ni-W/γ-Al_2O_3 catalysts

Catalyst	Loadings in catalyst preparation (wt.%)			Ni/(Ni + W) (at. ratio)	SBET (m^2/g)	Pore volume (ml/g)
	WO_3	NiO	Al_2O_3			
W	24.8	0.0	75.2	0.00	208	0.38
NiW (0.09)	24.8	0.8	74.4	0.09	202	0.36
NiW (0.17)	24.8	1.6	73.6	0.17	199	0.35
NiW (0.23)	24.8	2.4	72.8	0.23	200	0.36
NiW (0.29)	24.8	3.2	72.0	0.29	197	0.35
NiW (0.33)	24.8	4.0	71.2	0.33	190	0.34
NiW (0.41)	24.8	5.6	69.6	0.41	188	0.35
4NiW (0.50)	24.8	8.0	67.2	0.50	180	0.32
NiW (0.60)	24.8	12.0	63.2	0.60	172	0.29
Ni	0.0	5.6	94.4	1.00	–	–

For the samples of tungsten (alone) sulfided at 673 K, about 69% of the tungsten species is in the sulfided form. With the Ni content increasing from Ni/(Ni + W) = 0.17 to 0.60, the fraction of W^{4+} increases from 75 to 84%. Accordingly, the addition of Ni to the W phase induces both an increase of its dispersion (see next paragraph) as well as an augmentation of the sulfidability of the alumina-supported WO_x phase.

The Ni_{2p} peak at 853.7 eV is related to Ni in sulfided form [18,19]. For promoted NiW catalysts, it has been reported in [19] that two Ni species could coexist: one corresponding to pure Ni sulfide (at about 853.3 eV), and another

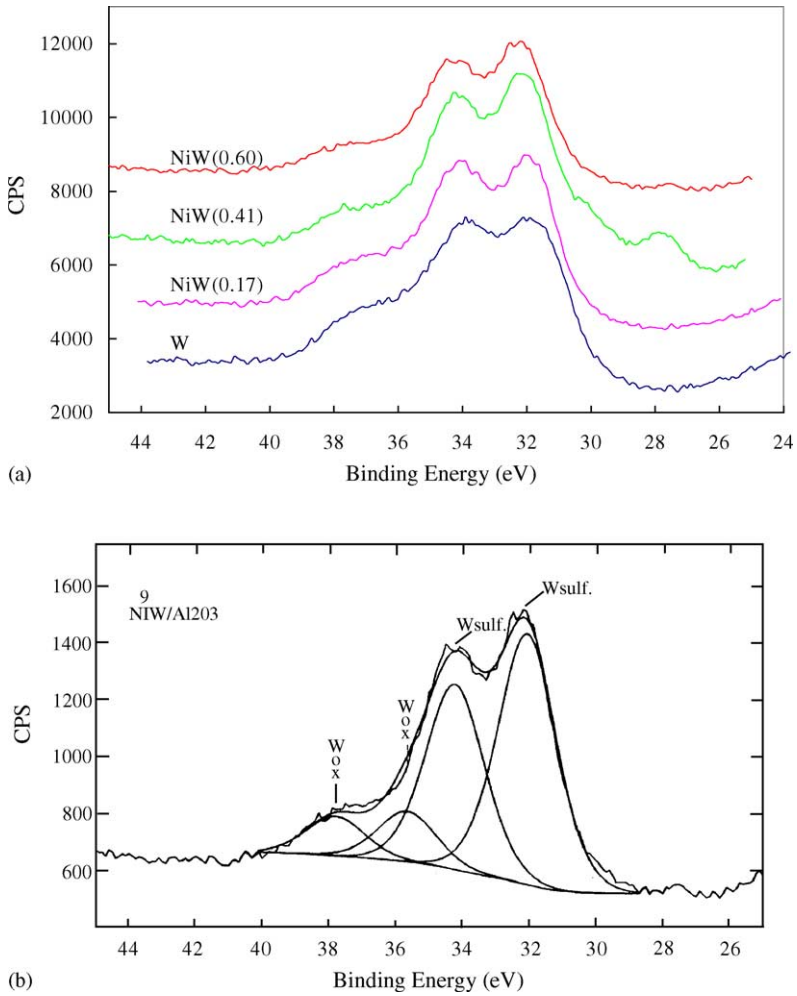

Fig. 1. (a) W_{4f} XPS spectra of NiW/γ-Al_2O_3 catalysts sulfided at 673 K. (b): Decomposition of the W_{4f} XPS spectra of NiW (0.60)/γ-Al_2O_3 catalyst sulfided at 673 K.

Table 2
Binding energies of sulfided NiW/Al_2O_3 catalysts

Catalyst	Binding energy (eV)			[FWH M]$_{Nipeak}$
	S_{2p}	$W4f_{7/2}$	$Ni2p_{3/2}$	
W	161.4	32.0	–	–
NiW (0.17)	161.6	32.0	853.7	2.99
NiW (0.41)	161.9	32.2	853.6	3.42
NiW (0.60)	161.9	32.2	853.4	3.77

Table 3
Sulfiding degree of W species in W/Al_2O_3 and NiW/Al_2O_3 catalysts

Catalyst	W oxide (%)	W sulfide (%)
W	31	69
NiW (0.17)	25	75
NiW (0.41)	20	80
NiW (0.60)	16	84

Ni species at higher binding energy attributed to the NiWS phase in which the Ni atom is a neighbor of the W atom and there is an electronic transfer from Ni atom to its environment. By comparison of the Ni_{2p} spectra of the three promoted catalysts it was observed that the Ni_{2p} peak of NiW (0.17) sample is more symmetric and the full width at half maximum (FWHM) is smaller (see values given in Table 2), which indicate that the Ni species present in this sample is almost completely in a NiWS state. The Ni_{2p} peaks broaden and slightly shifted to lower energies upon further Ni addition. This effect is more pronounced for the NiW (0.60) than for the NiW (0.41) one. This demonstrates that a Ni sulfide phase undoubtedly coexists with the NiWS on the NiW (0.60). The presence of such a separate NiS_x phase cannot be excluded on the NiW (0.41) since this sample presents a larger FWHM but the observed 0.2 eV binding energy shift is not high enough to reach a proper conclusion. Therefore, the XPS results suggest that Ni–W sulfide interaction species are preferentially formed with the addition of promoter Ni into W/Al_2O_3 catalyst at least up to $r = 0.41$.

3.2.2. Surface atomic ratios

The atomic ratios were calculated by integrating peak areas for each of the detected species. Information about the dispersion of the different phases was obtained by means of the ratios of W_{4f} and Ni_{2p} on Al_{2p} (Table 4). Initially, the W_{4f}/Al_{2p} ratio for the un-promoted sample is 0.059. This ratio increases up to 0.087 for $r = 0.17$ and remains constant for higher Ni loadings. Thus, we can infer that the addition of Ni favors the "dispersion" of W species. The Ni_{2p}/Al_{2p} ratio increases nearly linearly with the increase of Ni content in the catalysts up to $Ni/(Ni + W) = 0.6$. This implies that the Ni species have an excellent "dispersion" on the surface of the catalysts whatever the nature of the supported Ni sulfide phase.

3.3. TEM

3.3.1. Morphology of the active phases

Fig. 2 shows representative HREM views of four sulfided catalysts. The HREM views reveal the presence of typical structures of the layered WS_2 phase, which are homogeneously dispersed on the support. For the promoted catalysts, the WS_2 lattice fringes are to some extent more disordered.

3.3.2. Particle size measurement

Statistics over about 500 crystallites per catalyst sample were done in order to get a representative estimation of the average length and number of layers of the WS_2 crystallites in the different catalyst samples. The crystal size distributions are shown in Fig. 3a and b. For W catalyst, the average particle length is equal to 4.4 nm and the average layer number is equal to 2.3, whereas for promoted NiW catalysts, these two corresponding values are about 3.9 nm and 3, respectively. In spite that there are no big differences among these two statistical parameters for all promoted NiW catalysts, it is still obviously shown that upon increasing the content of promoter Ni, the number of layers increases gradually from 2.8 for NiW (0.17) catalyst to 3.2 for NiW (0.60) catalyst, and the length of slabs decreases, from 4.1 nm for NiW (0.17) catalyst to 3.8 nm for NiW (0.60). It should be noted that if the values of the stacking are closed to those recently reported by Vradman and Landau [20] for NiW/Al_2O_3 catalysts, the lengths of the particles are smaller, probably due to a lower tungsten amount.

3.4. Thiophene HDS

The influence of Ni loading on the activity of NiW catalysts in thiophene HDS is illustrated in Fig. 4. As expected, the result reveals that Ni leads to a strong promotional effect on the HDS activity. The optimum ratio of $Ni/(Ni + W)$ is about 0.4, the activity of the NiW (0.41) catalyst being about 30 times higher than that of the un-promoted one.

Table 4
Surface atomic ratios of sulfided catalysts

Catalyst	Surface atomic ratios by XPS					Loadings in preparation		
	W_{4f}/Al_{2p}	S_{2p}/Al_{2p}	$Ni2p_{3/2}/Al_{2p}$	Ni/(Ni + W)	S/(Ni + W)	W/Al	Ni/Al	Ni/(Ni + W)
W	0.059	0.13	0	0	2.20	0.072	0	0
NiW (0.17)	0.087	0.21	0.028	0.24	1.83	0.074	0.015	0.17
NiW (0.41)	0.085	0.22	0.078	0.47	1.35	0.078	0.055	0.41
NiW (0.60)	0.085	0.28	0.125	0.60	1.33	0.086	0.129	0.60

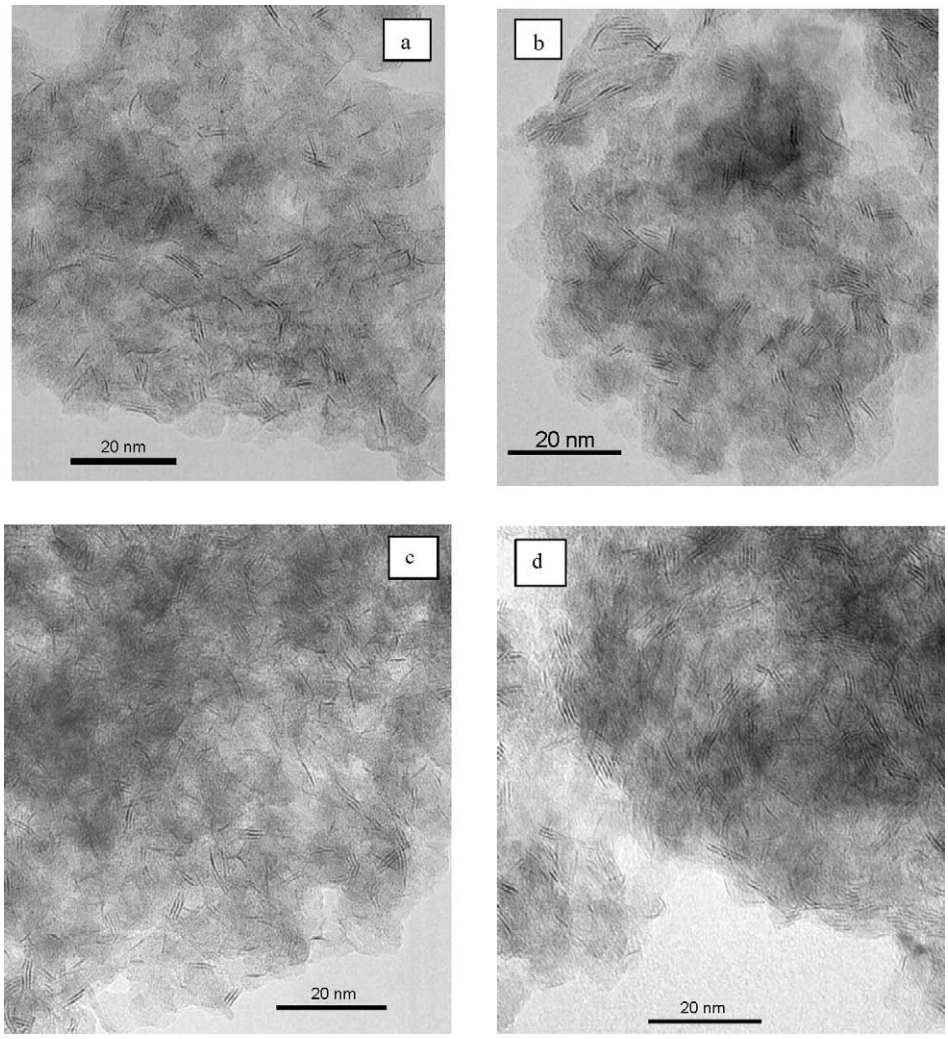

Fig. 2. TEM images of (a): W, (b): NiW (0.17), (c) NiW (0.41), and (d): NiW (0.60) catalysts sulfided at 673 K for 4 h.

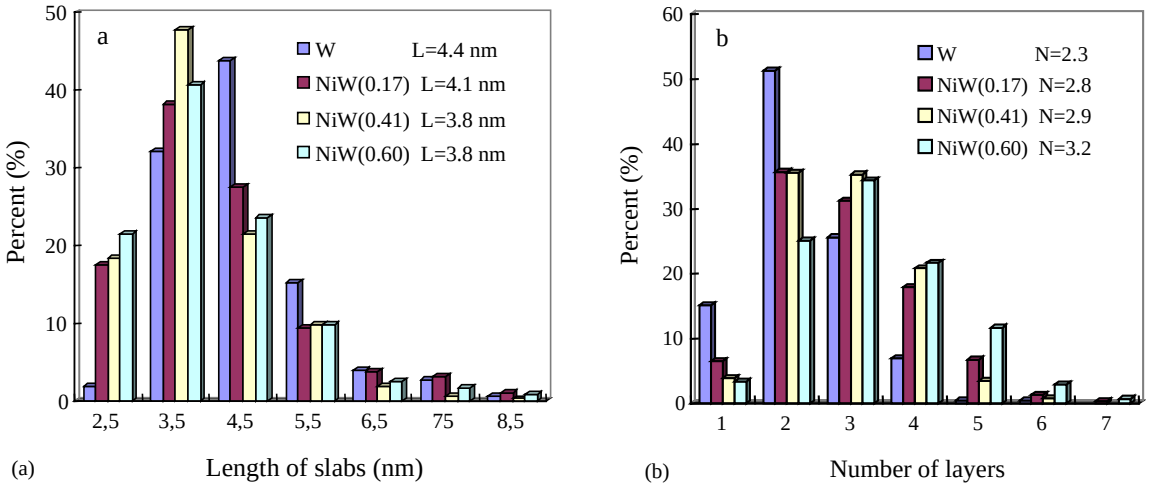

Fig. 3. Crystal size distribution of WS_2 for sulfided NiW/Al_2O_3 catalysts.

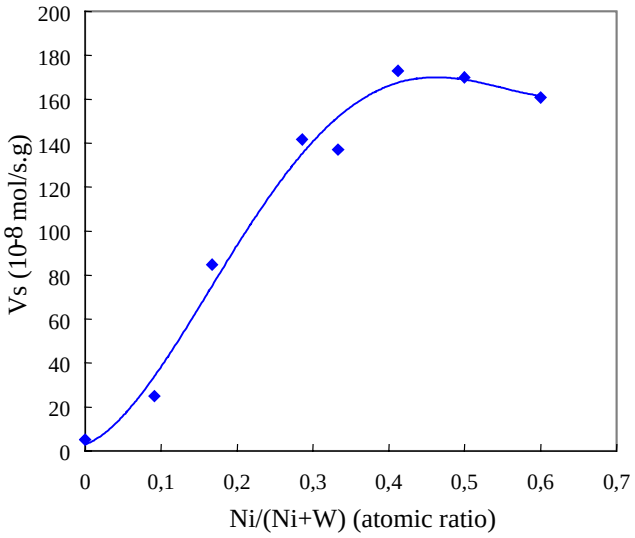

Fig. 4. Role of the promoter Ni on sulfided NiW/Al_2O_3 catalysts for thiophene HDS at 573 K.

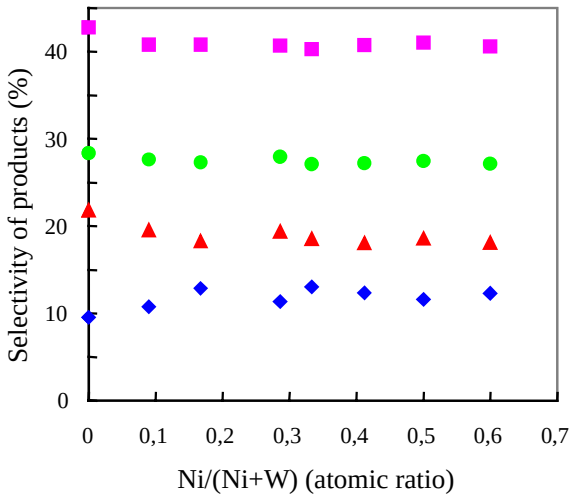

Fig. 5. Product distribution of thiophene HDS by sulfided NiW/Al_2O_3 catalysts at 573 K and a thiophene conversion of about 10%. (■), *trans*-2-butene; (●), *cis*-2-butene; (▲), 1-butene, and (◆), butane.

A nearly linear increase in activity is observed as far as the Ni/(Ni + W) atom ratio varies from 0 to 0.4. Further increase in Ni loading leads to a slightly decrease in activity. Fig. 5 provides the product distribution in thiophene HDS.

The observed products in the conversion of thiophene are regular HDS products such as *cis*-, *trans*-2-butene, 1-butene and *n*-butane. Negligible traces of *iso*-butane, *iso*-butene and tetra-hydrothiophene were also detected. The selectivities

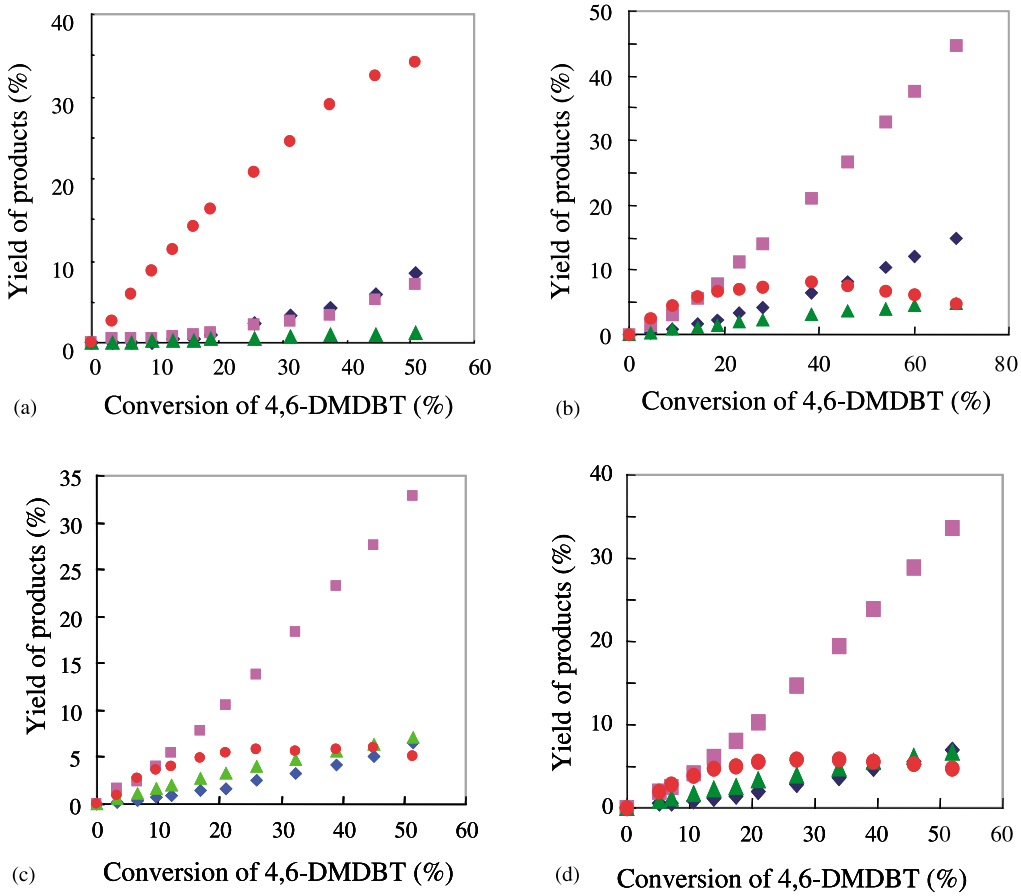

Fig. 6. Product distribution vs. conversion of 4,6-DMDBT over (a) W, (b)NiW (0.17), (c) NiW (0.41), and (d) NiW (0.60) catalysts. (■), DMCHB; (▲), DMBiPh; (◆), DMBCH, and (●), HN.

Table 5
Activity and selectivity of W/Al_2O_3 and NiW/Al_2O_3 for 4,6-DMDBT HDS

Catalyst	Activity			Selectivity			Promoting effect		
	A_T	A_{DDS}	A_{HYD}	S_{DDS}	S_{HYD}	DDS/HYD	Total	DDS	HYD
W	4.27	0.11	4.16	2.5	97.5	0.03			
NiW (0.17)	10.7	0.96	9.74	9.0	91.0	0.10	2.5	8.7	2.3
NiW (0.41)	10.6	1.73	8.87	16.3	83.7	0.19	2.5	15.7	2.1
NiW (0.60)	11.8	1.80	10.0	15.2	84.8	0.18	2.7	16.4	2.4

Note. $r = Ni/(Ni + W)$, A_T is the total activity, A_{DDS} is the activity for the DDS pathway, A_{HYD} the activity for the HYD pathway (10^{-5} mol s^{-1} kg^{-1}). S_{DDS} and S_{HYD} are selectivity (%) for DDS and HYD pathways, respectively. Conversion ≈ 10%.

for all main products on this series of catalysts are almost the same except for the un-promoted catalyst. These results may probably indicate that the nature of the active phase on all promoted NiW catalysts is similar.

3.5. 4,6-DMDBT HDS

The products of the transformation of 4,6-DMDBT are dimethylbiphenyl (DMBiPh), dimethyl-cyclohexylbenzene (DMCHB), dimethylbicyclohexane (DMBCH) and undesulfurized hydrogenated products such as tetrahydro-, and hexahydro-dimethyldibenzothiophenes. The yields of the different products can be plotted against the conversion as shown in Fig. 6, and allow us to calculate the product selectivities, which are given in Table 5 and illustrated in Fig. 7. For promoted catalysts, the main product is cyclohexylbenzene whereas for W (alone) catalyst, the most important products are undesulfurized hydrogenated products.

On all catalysts, promoted or not, HYD is the main transformation pathway. But there are great differences in the product distribution. On the un-promoted catalyst, more than 90% of the products are intermediates which are not desulfurized. On the promoted catalysts, the transformation reaction also prefers to occur by HYD pathway, whereas the final products are desulfurized products.

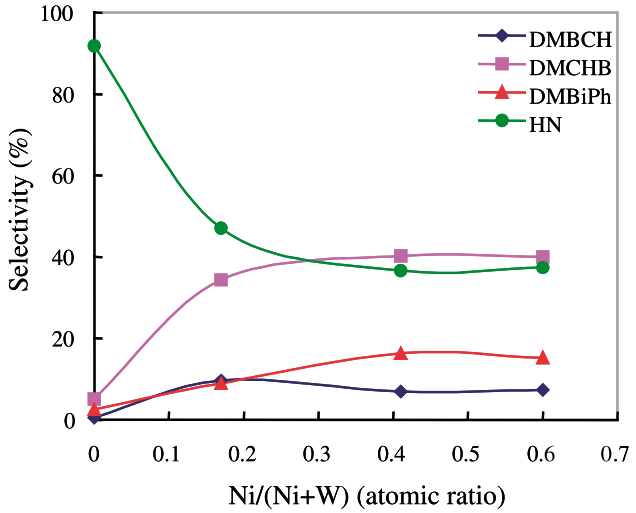

Fig. 7. Products distribution of W/Al_2O_3 and NiW/Al_2O_3 for 4,6-DMDBT HDS.

3.6. o-Xylene isomerization reaction

The main products in this reaction are: direct HYD products, isomerization products and hydrogenated products after isomerization as illustrated in Fig. 8. The HYD activity was therefore calculated according to the reaction of direct HYD, and the isomerization activity was based on the sum amount of products through isomerization pathway as well as followed by HYD, and the results are given in Table 6.

Table 6
Catalytic activity of NiW/Al_2O_3 catalysts in the isomerization of *o*-xylene

Catalyst	A_{tot}	A_{ISOM} (10^{-3} mol/g/h)	A_{HYD}	A_{ISOM}/A_{HYD}
W	0.64	0.48	0.16	3.0
NiW (0.17)	1.48	1.04	0.44	2.4
NiW (0.29)	2.36	1.70	0.66	2.5
NiW (0.41)	3.40	2.36	1.04	2.3
NiW (0.60)	3.38	2.35	1.03	2.3

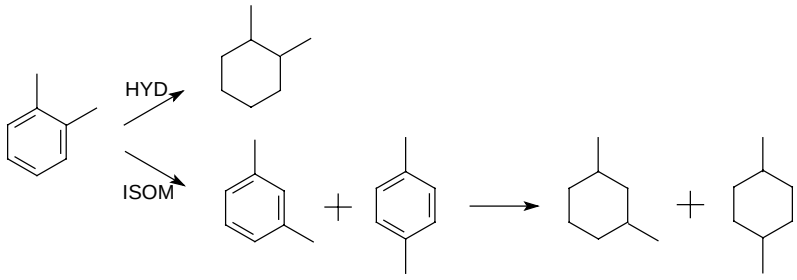

Fig. 8. Reaction scheme of *o*-xylene isomerization.

The total activity increases by a factor of five indicating an increasing acidity of the catalysts. The activities through ISOM and HYD pathways are enhanced proportionally to each other, resulting in almost constant A_{ISOM}/A_{HYD} ratios.

4. Discussion

The results obtained in the conversion of thiophene confirm the synergy generally observed in HDS reactions: the activity of the W/Al_2O_3 sample is improved upon addition of the promoter nickel. The maximum of activity is observed for a r ratio closed to 0.4 but does not vary a lot in the range 0.4–0.6. Such a composition is assumed to correspond to a complete occupation of the edges of the WS_2 slabs by the promoter according to the geometrical model of Kasztelean [21,22]. Moreover the activity of the best catalyst is 30 times higher than the un-promoted one, in agreement with previous data on tungsten-based hydrotreating catalysts [18].

Physico-chemical characterizations of the sulfided samples by TEM do not evidence any large variations in the morphology of the crystallites since the particles sizes only varied between 3.8 and 4.2 nm though the stacking of the layers is maintained between 2.3 and 3.2. Therefore, inside the geometrical model approach, such a large increase of HDS activity could not be explained solely by the variations of the number of edge sites. Indeed, more insight in the effect of the promoter could be obtained from XPS data. First of all, it appears that addition of Ni leads to some modifications in the sulfidability of the catalysts since the percentage of tungsten in the W^{4+} state increases from 70% in the absence of promoter to 80% at $r = 0.41$ when the maximum of activity is observed. Nevertheless no direct correlation seems to be drawn between such increase of activity and the observed variations of W^{4+}. However, XPS data also evidenced a continuous evolution of the Ni_{2p} peak binding energy with the nickel content. As discussed in the XPS results, binding energy of Ni in NiW (0.17) catalyst and symmetry of the peak indicate that Ni is mainly incorporated into a NiWS phase. At higher Ni content the Ni_{2p} peak is larger and shifts slightly to lower energy, which effect appears more pronounced for the NiW (0.6) sample in agreement with the progressive coexistence of a Ni sulfide phase with the NiWS phase.

Such an evolution of Ni species in the sulfided catalysts evidenced from XPS results, could be also correlated with catalytic activities in thiophene HDS. Nevertheless this reaction appears to be an easy one and changes in the selectivity are very slight. On the contrary, results on 4,6-DMDBT HDS illustrated in Figs. 6 and 7, are more interesting since large differences in products selectivities are noticed. Such variations have allowed us to propose that over such catalysts the reaction takes place through two parallel roads, one leading to biphenyl-type products and called "the direct desulfurization" pathway, and the second one leading to tetrahydro-dibenzothiophene-type products and cyclohexyl benzene type products and called the "hydrogenation" road ([5] and references therein). Such a mechanism has been reconsidered by Meille et al. [8] which proved that under classical HDS conditions the biphenyl is not converted into cyclohexylbenzene and that both biphenyl-type compounds and tetrahydro-dibenzothiophene-type compounds have a common dihydro-intermediate. This mechanism, schematized in Fig. 9 was later also considered by Bataille et al. [23] and by Hermann et al. [24] for 4,6-DMDBT transformation and by Macaud et al. [10] for various dialkyldibenzothiophenes.

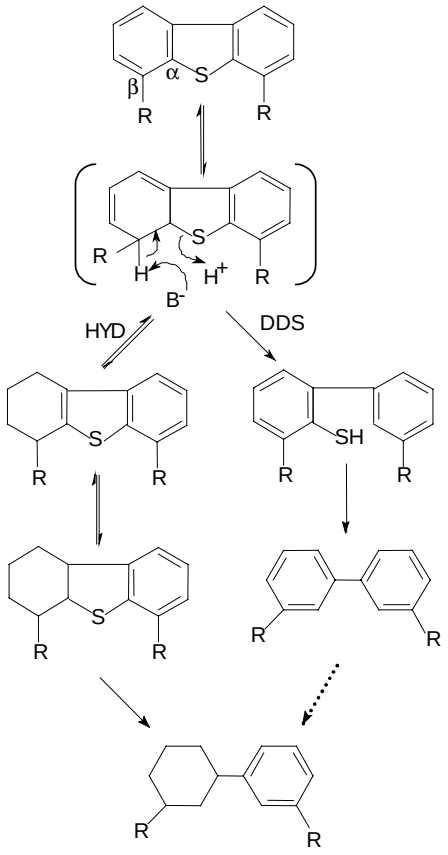

Fig. 9. Reaction scheme of alkyldibenzothiophene hydrodesulfurization.

In such a mechanism, after partial HYD of the alkyldibenzothiophene, the reaction could proceed via HYD or elimination (C–S bond rupture). According to Mijoin et al. [15] the orientation of the reaction (DDS road versus HYD road) could depend on the steric hindrance induced by alkyl groups, and on the basicity of the anions in the vicinity of the adsorbed dihydro-compound and the acidity of the SH group resulting in the heterolytic dissociation of H_2, these later points being strongly influenced by the promoter. Indeed, if the first proposal has been well demonstrated by some of us using various dialkyldibenzothiophenes [10], the second one is still to be completely demonstrated.

For sulfided catalysts, it is now accepted that the promoter increases the electron density on the sulfur atom, making such species more basic and therefore more active in the β

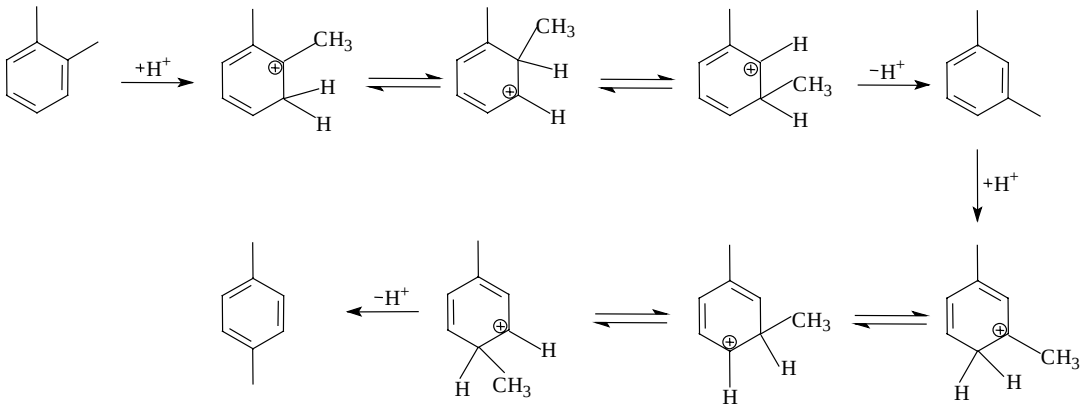

Fig. 10. Scheme of *o*-xylene isomerization into *m*-xylene and *p*-xylene.

elimination reaction (C–S bond rupture). Such a fact is well reflected by the greater effect of the promoter over the DDS reaction pathway than over the HYD one. However, in the same time there is a slight effect of the promoter on the HYD road. This is in agreement with the work of Berhault et al. [25] on pyridine and dimethyl-pyridine adsorption over Mo and CoMo silica supported catalysts. They found that the promoter does not increase significantly the number of sulfur vacancies, but drastically promotes the Bronsted acidity, leading to more dissociated hydrogen available for the reaction.

However such an increase of Bronsted acid site formation and consequently of active hydrogen species must be reflected in a reaction involving such entities. That could be the case for *o*-xylene isomerization which proceeds via a unimolecular mechanism involving transformation of benzenium ion intermediates through a methyl shift to form *m*-xylene and *p*-xylene on Bronsted acid site [26,27] as illustrated below in Fig. 10.

Indeed, results reported in Table 6 show a continuous increase of the xylene isomerization with the nickel content until a plateau of activity for nickel content higher than 0.41. If such an increase of the isomerization reaction could be due to an increase of Bronsted acid sites and therefore to H^+ entities, the heterolytic dissociation of H_2 leads to a parallel increase of H^- species and that must be reflected in a reaction involving such entities. That could be the case of HYD of an aromatic ring which was reported to proceed via successive addition of H^- and H^+ entities, the hydride addition appearing to be the rate limiting step [13]. Results of Table 6 effectively indicate a parallel increase of the HYD rate of *o*-xylene and of its isomerization. Such results could be considered as an indirect proof of the heterolytic dissociation of H_2 over these sulfided catalysts.

5. Conclusions

Ni addition to W/Al_2O_3 promotes remarkably the thiophene HDS activity and the optimum ratio was found for a $r = Ni/[Ni + W]$ ratio closed to 0.4. However TEM examinations of the sulfided samples indicated that such an increase of activity could not be correlated to variations in the morphology of the sulfide particles. XPS results show that at low $Ni/[Ni + W]$ ratio, Ni is mainly incorporated into "NiWS" phase though at high $Ni/[Ni + W]$ surplus Ni forms separate NiS phase.

For 4,6-DMDBT HDS, Ni addition is more effective over the C–S bond cleavage (elimination step) and such a selective promoting effect of Ni on DDS route can be ascribed to an increase of the basicity of the S^{2-} centers in the vicinity of the catalytic site which help H abstraction in the β position adjacent to the sulfur and therefore favors the β-elimination process. However, such variations in the acid–base properties of the sulfur anions led to an increase of hydrogen activation and consequently of Bronsted acid site formation, which was well reflected into *o*-xylene isomerization which proceeds via a mechanism involving transformation of benzenium ion intermediates through a methyl shift. Associated with 4,6-DMDBT HDS, this later reaction is useful to prove the effect of the promoter on acid–base properties of the catalysts.

Acknowledgements

This work was carried out in the framework of the French–Chinese joint laboratory (LFCC) between the Research Institute of Petroleum Processing of Beijing and the Institut de Recherches sur la Catalyse, UPR CNRS 5401. The authors thank the CNRS, the RIPP and the French Embassy to support this research. D. ZUO is greatly indebted to the French Ministry of Foreign Affairs and the French Embassy of Beijing for his Ph.D grant.

References

[1] M. Houalla, D. Broderick, A.V. Sapre, N.K. Nag, V.J.H. de Beer, B.C. Gates, H. Kwart, J. Catal. 61 (1980) 523.

[2] A. Amorelli, Y.D. Amos, C.P. Halsig, J.J. Kosman, R.J. Jonker, M. de Wind, J. Vrieling, Hydrocarbon Processing 71 (1992) 93.
[3] T. Kabe, A. Ishihara, H.A. Tajima, Ind. Eng. Chem. Res. 31 (1992) 1577.
[4] M.V. Landau, Catal. Today 10 (1991) 489.
[5] D.D. Whitehurst, T. Isoda, I. Mochida, Adv. Catal. 42 (1998) 345.
[6] G.F. Froment, G. A Depauw, V. Vanrysselberghe, Ind. Eng. Chem. Res. 33 (1994) 2975.
[7] R. Sanchez Delgado, "Organometallic modeling of the hydrodesulfurization and hydrodenitrogenation reactions", Catalysis by Metal Complexes, Vol. 24, Kluwer Academic, 2002.
[8] V. Meille, E. Schulz, M. Lemaire, M. Vrinat, J. Catal. 170 (1997) 29.
[9] K. Segawa, K. Takahashi, S. Satoh, Catal. Today 63 (2000) 123.
[10] M. Macaud, A. Milenkovic, E. Schulz, M. Lemaire, M. Vrinat, J. Catal. 193 (2000) 255.
[11] G.H. Singhal, R.L. Espino, J.E. Sobel, G.A. Huff, J. Catal. 67 (1981) 457.
[12] V. Meille, E. Schulz, M. Lemaire, M. Vrinat, Appl. Catal. A 187 (1999) 179.
[13] E. Olguin Orozco, M. Vrinat, Appl. Catal. A 170 (1998) 195.
[14] S. Kasztelan, D. Guillaume, Ind. Eng. Chem. Res. 23 (1994) 203.
[15] J. Mijoin, G. Perot, F. Bataille, J.L. Lemberton, M. Breysse, S. Kasztelan, Catal. Lett. 71 (3-4) (2001) 139.
[16] P. Da Costa, C. Potvin, J.M. Manoli, J.L. Lemberton, G. Perot, G. Djega-Mariadassou, J. Mol. Catal. A 184 (2002) 323.
[17] J. Mijoin, V. Thevenin, N. Garcia Aguine, H. Yuze, J. Wang, W.Z. Li, G. Perot, J.L. Lemberton, Appl. Catal. A 180 (1999) 95.
[18] M. Breysse, C. Gachet, L. de Mourgues, Catalytic hydrotreatment on alumina supported NiW sulfides, Catal. Today 4 (1) (1988) 39.
[19] W. Eltzner, M. Breysse, M. Lacroix, M. Vrinat, Polyhedron 5 (1–2) (1986) 203.
[20] L. Vradman, M.V. Landau, Catal. Lett. 77 (1–2) (2001) 47.
[21] S. Kasztelan, H. Toulhoat, J. Grimblot, J.P. Bonnelle, Appl. Catal. 13 (1984) 127.
[22] S. Kasztelan, Catal. Lett. 2 (1989) 165.
[23] F. Bataille, J.L. Lemberton, P. Michaud, G. Pérot, M. Vrinat, M. Lemaire, E. Schulz, M. Breysse, S. Kasztelan, J. Catal. 191 (2000) 409.
[24] N. Hermann, M. Brorson, H. Topsoe, Catal. Lett. 65 (2000) 169.
[25] G. Berhault, M. Lacroix, M. Breysse, F. Mauge, J.C. Lavalley, H. Nie, L. Qu, J. Catal. 178 (1998) 555.
[26] S. Morin, P. Ayrault, S.E. Mouahid, N.S. Gnep, M. Guinet, Appl. Catal. A 159 (1997) 317.
[27] J.W. Ward, R.C. Hansford, J. Catal. 119 (1989) 252.